Near-Net Shapes Al_2O_3–SiC_w Ceramic Nanocomposites Produced by Hybrid Spark Plasma Sintering

E. Kuznetsova, P. Peretyagin, A. Smirnov, W. Solis and R. Torrecillas

Abstract This article describes the process and demonstrates the possibility to obtain a complex square-shaped nanostructured ceramic cutting composite by spark plasma sintering. Microstructure, mechanical, and wear properties of complex shape inserts were studied and compared with the properties of inserts which were cut from the SPS-sintered cylinder by diamond disk. Both types of inserts exhibited similar properties, meanwhile, fabrication of complex-shaped sample is less expensive and time-consuming process due to the absence of diamond disk cutting operation.

Keywords Spark plasma sintering · Complex shape · Cutting tools
Ceramic composites · Al_2O_3–SiC_w

E. Kuznetsova · P. Peretyagin (✉) · A. Smirnov · W. Solis · R. Torrecillas
Laboratory of Electric Currents and Sintering Technologies (LECAST),
Moscow State University of Technology "STANKIN", Moscow, Russian Federation
e-mail: p.peretyagin@stankin.ru

E. Kuznetsova
e-mail: ev.kuznetsova@stankin.ru

A. Smirnov
e-mail: a.smirnov@stankin.ru

W. Solis
e-mail: washsolis@gmail.com

R. Torrecillas
e-mail: r.torrecillas@stankin.ru; r.torrecillas@cinn.es

R. Torrecillas
Nanomaterials and Nanotechnology Research Centre (CINN),
CSIC-Universidad de Oviedo, Madrid, Spain

K.V. Anisimov et al. (eds.), *Proceedings of the Scientific-Practical Conference "Research and Development - 2016"*, https://doi.org/10.1007/978-3-319-62870-7_42

Introduction

Spark plasma sintering is a high-speed powder consolidation/sintering technology capable of processing a wide variety of conductive and nonconductive materials [1]. The main advantage of the spark plasma sintering technique is very high heating and cooling rates that allow to produce highly dense traditionally difficult-to-sinter materials. A wide range of material types such as nanostructured materials [2], functional-graded materials [3], hard alloys [4], titanium alloys [5], bioceramics [6], porous materials [7] for various applications was fabricated by spark plasma sintering.

Specimens produced by spark plasma sintering have shown improvements in microstructure (including decreased grain growth) [8] corrosion resistance [9], and mechanical properties [10], compared to conventional methods. On the other hand, wide application of the spark plasma sintering in industrial field is limited due to the extreme difficulty inobtaining near-net-shape ceramic samples. Ceramic cutting inserts are one of the examples of complex shape material. Previous research showed enhancement of endurance limit and reduction of the probability of catastrophic failure in ceramic cutting inserts produced by spark plasma sintering compared to conventional ones. This behavior was explained by the lower grain size and homogeneous microstructure of spark plasma sintering sintered ceramic cutting inserts. The main problem of sintering samples of complex shape is to design special molds and technological processes of consolidation to obtain the desired homogeneity of the microstructure and, consequently, physical and mechanical properties of the sintered sample. At present, typical spark plasma-sintered samples have a cylindrical shape and should be machined after sintering. Nevertheless, the high hardness and brittleness of ceramics make machining very difficult or even impossible.

Therefore, the solution proposed in this paper, to create a special graphite mold and sinter ceramic cutting inserts with square shape. In addition, in order to compensate thermal gradients of spark plasma sintering additional heating system was used. This hybrid system leads to enhanced sintering behavior with optimized homogeneity.

The objective of the present work was to investigate the sintering behavior of ceramic cutting inserts with square shape and study microstructure and mechanical properties of sintered samples.

Materials, Methods, and Characterization

Modeling

Numerical modeling was performed by finite element method of the SPS Al_2O_3–SiC_w samples in the form of square plates SNGN standard geometry. The temperature

distribution and mechanical stresses in the sample and in the mold were obtained. Numerical modeling was performed using the software COMSOL Multiphysics.

The properties of materials—graphite, alumina, and silicon carbide were obtained from standard materials library of COMSOL Multiphysics software.

Numerical simulations were performed by solving the dual problem of thermoelectric and static loading in the COMSOL Multiphysics software. The thermoelectric task of heating sample was solved using a special module Joule heating. The task of modeling the stress–strain state of the system at the applications of static loads to the upper punch size of 100 MPa for 120 s was solved in the Solid Mechanics module of the COMSOL Multiphysics software.

Raw Materials

Al_2O_3–SiC_w was used of Ceramtuff (grade HA9S) "*ready-to-press powder*", a commercial blend of alumina (Al_2O_3) powder and 17 vol.% of silicon carbide whiskers (SiC_w), fabricated by the company Advanced Composite Materials, LLC (Greer, SC, USA), was chosen for the production of ceramic-graphene composites. The typical properties of HA9S after sintering by hot press at 1850 °C are presented in Table 1.

Spark Plasma Sintering

Powder densification was performed by SPS (FCT Systeme GmbH, KCE FCT-H HP D-25 SD, Rauenstein, Germany) at a maximum temperature of 1780 °C, reached under vacuum at a heating rate of 100 °C/min, and an applied pressure of 80 MPa. The final temperature and pressure were maintained for 3 min. Sintering temperature was chosen based on a previous study [11].

Table 1 Properties of the Ceramtuff blend after densification

Density (% φ_{th})	Flexural strength (MPa)	Young modulus (GPa)	Hv (GPa)	K_{IC} (MPa $\sqrt{m}$)	Thermal conductivity (W/m K)	Thermal shock resistance ΔT (°C)	Coefficient of thermal expansion (10^{-6}/°C)
99	550–700	400	20.7	7–9	35	1000	6.8

Microstructural Characterization

Scanning electron microscopy (SEM) characterization was carried out on polished down to 1 μm and thermally etched surfaces (1250 °C for 3 min) by VEGA 3 LMH (SEM Tescan, Brno, Czech Republic). The density of the sintered samples (ρ) was measured in distilled water using Archimedes' principle and was compared with the theoretical value, calculated according to the rule of mixtures.

Mechanical Properties

Vickers hardness, Hv, was measured on polished surfaces using a Vickers diamond indenter (QNess A10 Microhardness Tester, Salzburg, Austria), applying a load of 98 N and an indentation time of 10 s. The magnitude of the Vickers hardness was determined according to:

$$Hv = 0.1891P/d^2, \tag{1}$$

where P is the applied load (in N) and d is the average length of the two diagonals (in mm). The sizes of the corresponding indentations were determined via SEM. The hardness results were averaged over 10 indentations per specimen.

Fracture toughness (K_{1c}) was measured using single edge notched beams (SENB, dimension 3.0 × 4.0 × 45 mm^3). Tests were performed at room temperature, using the same testing machine applied for flexural strength determination, at a crosshead speed of 0.5 mm/min with a span of 40 mm. Specimens were notched with a diamond blade saw. The method and formulas for calculating K_{1c} have been reported elsewhere [12].

Machining Testing Conditions

The efficiency of cutting tools is determined by measuring wear occurring on the contact surface between the tool and the machined material. It is important to note that the wear observed in the tool depends on the properties of the tool material as well as the machined material, but also on wear testing conditions.

As a criterion of quality of the cutting inserts was chosen the wear of its rear surface, which occurs the turning of cylindrical samples of X8NiCrAlTi32-21 ISO 4955 heat-resistant steel.

The longitudinal turning of steel specimens was performed with the following testing conditions: cutting speed V = 300 m/min and traverse S = 0.15 mm/rev, depth of cut t = 0.5 mm. The maximum limit in wear on the backside of the cutting edge of ceramic materials was taken to be h = 0.5 mm, as higher values are

considered as catastrophic wear, Outbreaks of wear plates were observed and measured with an optical microscope Zeiss discovery v12.

For comparison purpose, inserts from standard disk Al_2O_3–SiC_w SPS samples were also used.

Results and Discussion

Figure 1a, b shows the FEM modeling results. Figure 1c exhibits a square cross sectional near-net shape spark plasma sintering graphite die for ceramic inserts fabrication. Figure 2 shows the SEM micrographs of a fracture surface of (a) standart disk-shaped and (b) near-net shape samples of the Al_2O_3-SiC_w ceramic composites sintered by SPS.

The theoretical density for the composite of Al_2O_3 matrix with 17 vol.% of SiC whisker reinforcements was calculated, and its value is ρ_{teor} = 3.86 g/cm^3. The measured density of the sintered samples was 3.83 ± 0.1 g/cm^3, and this value is

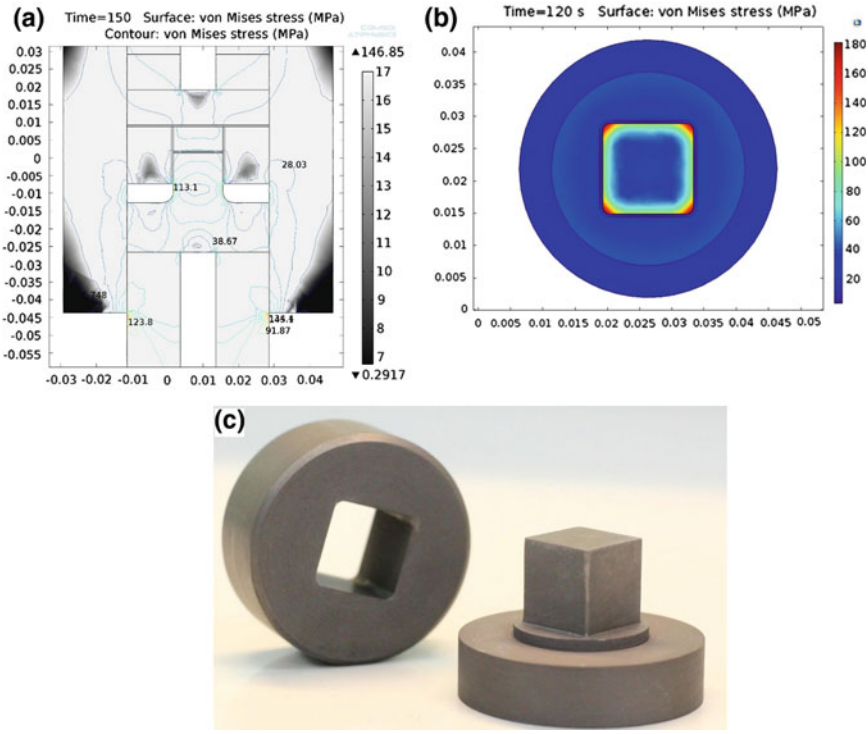

Fig. 1 The FEM modeling results and (**a**), (**b**), and near-net shape graphite mold (**c**)

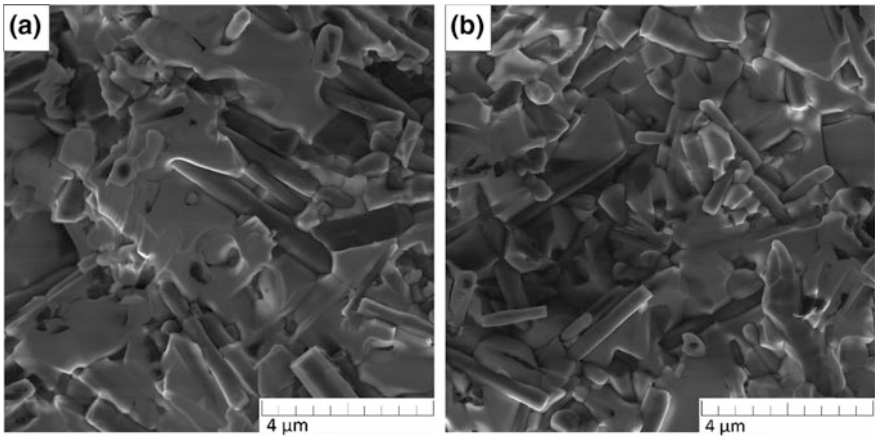

Fig. 2 SEM micrograph of the fracture surface of the standard disk Al_2O_3–SiC_w composites (**a**) and near-net shape Al_2O_3–SiC_w composites (**b**)

the 99.2% of the theoretical. This value indicate the possibility of obtaining density material by the using molds with square cross section.

The sintered samples' hardness and the fracture toughness were measured in three different regions of the cross section, from the periphery to the center, in order to determine the presence of possible mechanical properties' anisotropy caused by temperature gradients during SPS process (Table 2).

The hardness values of two different cross sections do not change significantly between the three different regions and this indicates that the properties in the volume of the material are practically the same for both cases (Table 2); moreover, it confirms a uniform distribution of the heat on the sample during the sintering process.

The average fracture toughness of the samples with circular and square cross sections are 7.82 and 7.74 MPa $m^{1/2}$ respectively. These values of hardness and fracture toughness are higher than the common values of samples obtained by conventional sintering methods. Analysis of fractured surfaces shows a uniform distribution of silicon carbide fibers throughout the volume for the samples with different cross sections (Fig. 2a, b).

Figure 2b shows that, in the structure, the grains have different sizes, but there are no abnormally large dimensions. Thereby, with a selection of the optimal

Table 2 Properties of the composites with different molds design

	Density (% φ_{th})	Hardness, Hv	Toughness, K_{IC} (MPa $\sqrt{m}$)	Life time of cutting inserts, τ, s	Wear major flank, h (mm)
Standard disk	99	2165	7.80	2.8	0.51
Near-net shape	99	2198	7.83	3	0.48

parameters for the hybrid SPS process we were able to obtain a uniform microstructure in the sintered ceramic sample with a complex shape.

The machining test shows (Table 2) that the tool life of the ceramic cutting inserts with a complex shape (square cross section) was 2.8 min, and the tool life for the inserts obtained from the sample with circular section was 3 min. These results indicate that the tool life of the sample with the square cross section is not much different from the second sample.

It should be noted that properties of the ceramic cutting inserts with complex shape were achieved by pre-selecting the optimum geometrical parameters of the graphite die for the SPS equipment, which provide a uniform temperature gradient in the volume of the sintered sample.

Conclusion

Fully dense and homogeneous Al_2O_3–SiC_w square-shaped ceramic composites have been successfully fabricated by Hybrid Spark Plasma Sintering. No significant differences in hardness (2209 HV) and fracture toughness values (7.82 MPa $m^{1/2}$) were found in comparison with the composites produced from traditional SPS sintered cylindrical samples by diamond cutting. Therefore, SPS graphite mold with complex shape offers multiple advantages over traditional cylindrical forms and enables advanced ceramic materials to be intricately shaped with required accuracy and machining cost reduction.

Acknowledgements Research are carried out with the financial support of the state represented by the Ministry of Education and Science of the Russian Federation. Agreement no. 14.577.21.0089 22.June 2014. Unique project Identifier: RFMEFI57714X0089.

References

1. Risbud, S.H., Han, Y.-H.: Preface and historical perspective on spark plasma sintering. Scr. Mater. **69**, 105–106 (2013)
2. Nygren, M., Shen, Z.: Novel assemblies via spark plasma sintering. Silic. Indus. **69**, 211–218 (2004)
3. Watari, F., Yokoyama, A., Omori, M., Hirai, T., Kondo, H., Uo, M., Kawasaki, T.: Biocompatibility of materials and development to functionally graded implant for bio-medical application. Compos. Sci. Technol. **64**, 893–908 (2004)
4. Zhang, F., Shen, J., Sun, J.: The effect of phosphorus additions on densification, grain growth and properties of nanocrystalline WC–Co composites. J. Alloys Compd. **385**, 96–103 (2004)
5. Zhang, F., Weidmann, A., Nebe, J.B., Beck, U., Burkel, E.: Preparation, microstructures, mechanical properties, and cytocompatibility of TiMn alloys for biomedical applications. J. Biomed. Mater. Res. B. **94B**, 406–413 (2010)
6. Gu, Y.W., Khor, K.A., Cheang, P.: Bone-like apatite layer formation on hydroxyapatite prepared by Spark Plasma Sintering (SPS). Biomaterials **25**, 4127–4134 (2004)

7. Zhang, F., Otterstein, E., Burkel, E.: Spark plasma sintering, microstructures, and mechanical properties of macroporous titanium foams. Adv. Eng. Mater. **12**, 863–872 (2010)
8. Han, Y.H., Nagata, M., Uekawa, N., Kakegawa, K.: Eutectic Al_2O_3–$GdAlO_3$ composite consolidated by combined rapid quenching and spark plasma sintering technique. Brit. Ceram. Trans. **103**, 219–222 (2004)
9. Yue, M., Zhang, J.X., Liu, W.Q., Wang, G.P.: Chemical stability and microstructure of Nd-Fe-B magnet prepared by spark plasma sintering. J. Magnetism Magnet. Mater. **271**, 364–368 (2004)
10. Nygren, M., Shen, Z.: On the preparation of bio-, nano- and structural ceramics and composites by spark plasma sintering. Solid State Sci. **5**, 125–131 (2003)
11. Gutiérrez-González, C.F., Suarez, M., Pozhidaev, S., Rivera, S., Peretyagin, P., Solís, W., Díaz, L.A., Fernandez, A., Torrecillas, R.: Effect of TiC addition on the mechanical behaviour of Al_2O_3–SiC whiskers composites obtained by SPS. J. Eur. Ceram. Soc. **36**, 2149–2152 (2016)
12. Smirnov, A., Bartolomé, J.F.: Mechanical properties and fatigue life of ZrO_2-Ta composites prepared by hot pressing. J. Eur. Ceram. Soc. **32**(15), 3899–3904 (2002)